Photoinduced dynamics of CO on Ru(0001): Understanding experiments by simulations with all degrees of freedom

Bruno Mladineo,[1] J. Iñaki Juaristi,[2,3,4] Maite Alducin,[3,4] Peter Saalfrank,[5] and Ivor Lončarić[1]

[1])*Ruđer Bošković Institute, Zagreb, Croatia*

[2])*Departamento de Polímeros y Materiales Avanzados: Física, Química y Tecnología, Facultad de Químicas, Universidad del País Vasco (UPV/EHU), Donostia-San Sebastián, Spain*

[3])*Centro de Física de Materiales CFM/MPC (CSIC-UPV/EHU), Donostia-San Sebastián, Spain*

[4])*Donostia International Physics Center DIPC, Donostia-San Sebastián, Spain*

[5])*Universität Potsdam, Institut für Chemie, Potsdam-Golm, Germany*

(*Electronic mail: ivor.loncaric@gmail.com)

(Dated: June 20, 2025)

Real-time pump-probe experiments are powerful tools for monitoring chemical reactions but often need parallel theoretical modelling to disentangle different contributions. Monitoring X-ray spectra of photoinduced dynamics of CO on Ru(0001) provided a strong indication for a transient "precursor state" of unidentified nature, to various subsequent outcomes. So far, the precise nature of the postulated precursor remained elusive also in state-of-the-art ab initio molecular dynamics models including single-moving CO molecules. In the present work, we have constructed a density functional theory-based machine learning interatomic potential energy surface that is valid for all ionic degrees of freedom of the system, comprising many molecules at various coverages and moving surface atoms. Our Langevin dynamics with electronic friction based on the new potential energy surface identified the precursor state as dynamically trapped molecules around 6 Å from the surface that arise from adsorbate-adsorbate interactions. We have compared our results to experimental observations and calculated the dependence of reaction probabilities on pump laser fluence and initial surface coverage.

I. INTRODUCTION

Pump-probe experiments with ultrashort laser pulses allow monitoring dynamics, breaking and forming chemical bonds, in real time providing valuable insights into chemical reactions or non-reactive events. Of particular importance are reactions of molecules on metal surfaces as elementary steps of heterogeneous (photo-)catalysis. Prototypical experiments for real-time monitoring of photoinduced dynamics of molecules on surfaces were performed for CO on Ru(0001).[1,2] In the first experiment,[1] using a free-electron X-ray laser probe, oxygen-resonant time-resolved X-ray emission spectroscopy (XES) and X-ray absorption spectroscopy (XAS), were used to monitor the dynamics of CO after an initial, femtosecond-laser pump pulse with a wavelength of 400 nm and fluence of 140 J/m^2. Observed shifts in the X-ray spectra point out to a significant bond weakening between CO and the Ru surface. By comparing to a calculated potential of mean force,[1] it was suggested that the experiments can be explained by CO molecules populating a so-called precursor state – a state where molecules are trapped relatively far from the surface.

In a subsequent experiment,[2] two different optical pump fluences were used (100 J/m^2 and 140 J/m^2). It was shown that in the case of lower fluence of 100 J/m^2, O-resonant time-resolved XES and XAS signals differ from those at the higher fluence of 140 J/m^2. By averaging spectra over the delay range between 2 and 15 ps, stronger CO-metal π interactions were observed for 100 J/m^2 in contrast to apparent CO-Ru bond weakening observed for 140 J/m^2. Real-time monitoring of spectra has shown that at short times ($<$2 ps) after the pump pulse for both fluences there is an increase in bonding strength, but between 2 and 4 ps, for the fluence of 140 J/m^2, bonding weakens, which was explained by the population of the above-mentioned precursor state.

A more detailed study, using polarized free-electron laser pulses[3] studying the C K-edge in the X-ray absorption spectrum showed that CO molecules in the precursor state rotated freely and resided on the surface for several picoseconds. Moreover, an additional resonance was identified and attributed to CO molecules residing at bridge/hollow sites.

Theoretical calculations have not yet been able to capture this precursor state unambiguously, nor its precise nature. In Ref. 1, to corroborate experiments, a simple potential of mean force model was used to explain the precursor state and indeed a separate physisorption well in addition to a deep chemisorption well was proposed. However, the entropy-driven barrier that gives rise to the precursor state was a result of oversimplification of the underlying potential energy surface as shown in Ref. 4. In that reference, a detailed dynamics study was performed for a single moving CO molecule (repeated periodically with a 2×2 unit cell) based on a density functional theory (DFT) derived six-dimensional potential energy surface. The dynamics showed no trapping in a precursor state and direct lateral diffusion or desorption instead.[4] These dynamics were based on a well-established methodology[5,6] where a pump pulse excitation is modelled by a two-temperature model (2TM) providing time-dependent electronic and lattice surface temperatures. Dynamics are based on the Langevin equation, which includes electronic friction calculated in local density friction approximation (LDFA)[7] and random forces due to the electronic temperature acting on the molecule. It has been shown that the LDFA model provides a good balance between accuracy and computational feasibility for frictional molecular dynamics even on d-band metals, in particular if no mode-selective processes are considered.[8,9] The lattice temperature and lattice motion (phonons) were approximately included by coupling molecular degrees of freedom to a generalized Langevin oscillator.[10,11]

While no precursor state was found with this six-dimensional model (all degrees of freedom of single CO molecule on the surface), a number of other experimental observations were well reproduced.[4] In particular, an observed power-law behaviour of the desorption yield as a function of laser fluence was similar to the experimental one[12] and two-pulse correlation experiments were reproduced validating the model. Furthermore, simulations of molecular beam experiments[13] with the same six-dimensional potential energy surface were in full agreement with experiments that show large sticking probabilities of CO to Ru(0001) at low incidence energies and, therefore, no existence of a barrier to the chemisorbed state.

Since the model with a single moving molecule is apparently not able to provide a theoretical explanation for the experimental observations related to the experimentally suggested precursor state, we postulate that adsorbate-adsorbate interactions are crucial. With the development of DFT-based machine learning interatomic potentials, it has become possible to treat all degrees of freedom with DFT accuracy, including the movement of surface atoms and modelling many adsorbates on the surface with changing coverages.[14–19] To test our hypothesis, we have developed a full-dimensional potential energy surface for CO/Ru(0001) valid for varying coverages that enabled us to study the paradigmatic, but still unexplained ultrafast photoinduced dynamics of CO on Ru(0001). Based on the new machine learning potential energy surface, we show that our Langevin dynamics model reproduces a precursor state that arises as a consequence of adsorbate-adsorbate interactions.

II. MODELS AND METHODS

A. Machine learning interatomic potential

A machine learning interatomic potential was trained with the Allegro architecture, a many-body neural network (NN) potential based on the NequIP[20] architecture that uses iterated tensor products of learned equivariant representations to bypass the atom-centered message passing.[21] Using hyperparameter optimization, we explored the impact of cutoff radius on accuracy and performance, and settled on a cutoff radius of 6 Å . Other important hyperparameters are the number of Allegro layers which is set to 3 and the environment embedding multiplicity set to 32. Other hyperparameters can be found in the uploaded training script in the supplementary material. The total number of data points in the training set is composed of 9762 structures with corresponding energies and forces with a 90/10 training/validation split. Mean absolute errors of the model are 5.2 meV/atom for energy and 5.8 meV/Å for forces.

To construct the dataset, we have used molecular dynamics calculations based on periodic density functional theory (DFT) for canonical ensembles at various temperatures. For this, we used the VASP 6.3.1[22,23] code and its on-the-fly machine learning capability[24] that through the use of Bayesian-learning algorithm can efficiently estimate uncertainties and sample the configurational space. To collect data, we have run velocity rescaling dynamics with temperatures increasing from 300 K to 3000 K and with different numbers of molecules on the surface representing coverages from 0.11 ML to 2 ML (we have used 1, 2, 3, 6, 9, and 18 molecules on a 3×3 surface cell). For all DFT calculations we have used 3×3 Ru(0001) surface cell with lattice parameter of 2.75 Å , 5 layers in the slab and 20 Å of space between periodic slab images. We have used $4{\times}4{\times}1$ Γ-centered **k**-point Monkhorst-Pack mesh, a 400 eV energy cut-off for plane waves, and 0.2 eV as a width of Methfessel-Paxton smearing. For the exchange-correlation functional we have used the so-called vdW-DF functional of Dion et al.[25] that provides van der Waals type interactions and was found to give accurate predictions for CO/Ru(0001).[26]

B. Langevin dynamics

We have run dynamics for three different coverages, 0.33, 0.58, and 0.66 ML (monolayers) as shown in Fig. 1 a)-d). Starting geometries for 0.33 and 0.58 ML are scanning tunnelling microscopy-determined structures from Ref. 27, while the starting geometry for 0.66 ML is taken

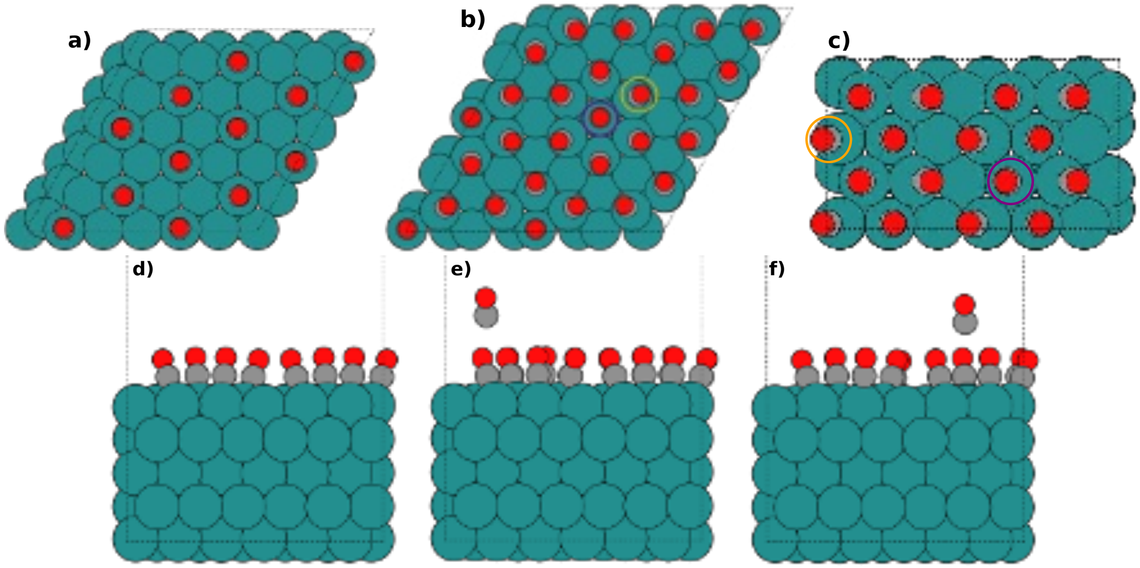

Figure 1: a)-c) Starting supercell geometries used for the dynamics shown as top-down views for a) 0.33 ML, b) 0.58 ML, and c) 0.66 ML coverages. CO molecules adsorb with C (grey) down and O (red) up on Ru (green). d)-f) Side view of the 0.66 ML supercell for the following configurations: d) starting geometry shown in c), e) the CO molecule noted with a yellow circle in c) adsorbed in the physisorption well, and f) CO molecule noted with purple circle adsorbed in the physisorption well.

from Ref. 28. Structures shown in Fig. 1 a)-d) are optimized with our potential. For 0.58 ML, tilting of molecules noted with a yellow circle is 14°, which compares well with the experimental value of 15°. Electronic and phonon temperatures were obtained from a two-temperature model with ruthenium parameters as in previous works.[4] The laser pulse shape is Gaussian, the pulse duration is 50 fs (FWHM), the wavelength is 400 nm, and the initial temperature is 300 K as in experiments.[2,4] Solutions of the two-temperature model for a fluence of 100 and 140 Jm^{-2} are shown in Figs. S1 and S2 (found in the supplementary material), together with obtained adsorbate and surface temperatures. For atomic friction coefficients (for C and O), which enter the Langevin equations to be solved, we use the same fit as in our previous works.[4,13,29] The friction coefficients depend on electronic densities provided by the bare surface. The latter was obtained in the current work as a sum of contributions of individual Ru atoms as in Ref. 17, with the following function (in atomic units, a_0 is the Bohr radius) fitted to the DFT denisty of the bare surface with the same computational set-up:

$$\rho_{el}(\vec{r}) = 0.91973286 a_0^{-3} \times \sum_{\mathrm{Ru}} \exp(-2.86725188 a_0^{-1} \times \sqrt{(\vec{r}-\vec{r}_{\mathrm{Ru}})^2}) \tag{1}$$

where the ρ_{el} is the electron density and $\sqrt{(\vec{r}-\vec{r}_{\mathrm{Ru}})^2}$ is the distance to any Ru atom. A comparison between DFT and fitted electronic densities is shown in Fig. S3. The surface temperature was set to the obtained phonon temperature via the Langevin thermostat with the friction parameter set to 0.2, as implemented in the Atomic Simulation Environment.[30] The timestep for the integration was set to 0.5 fs. We have integrated each trajectory for 50 ps and for each initial condition we run between 200 and 467 trajectories such that number of treated CO molecules is ≈ 5600.

III. RESULTS

We start by exploring the one-dimensional potential energy curves of a single CO molecule desorbing from Ru(0001) for different coverages as shown in Fig. 2. The energy as a function of the distance between the CO centre of mass (COM) and the average height of the surface Ru atoms is obtained such that the C atom of the chosen CO molecule and the bottom layer of the Ru slab are fixed with other coordinates allowed to relax for different C atom distances from the surface. The desorption energy from the chemisorption well for a coverage of $\approx$0 ML [single molecule in 6×6 Ru(0001) cell] is 1.59 eV, in accordance with previous calculations.[26] As coverage increases, the desorption energy decreases to 1.50 eV for a coverage of 0.33 ML, 1.20–1.29 eV for 0.58 ML, and 1.04–1.16 eV for 0.66 ML. For coverages of 0.58 and 0.66 ML there are two inequivalent CO molecules [noted with yellow and purple circles in Fig. 1 b) and c)] resulting in different potential energy curves. Experimentally,[31] desorption energy for low coverages is 1.6–1.7 eV, decreasing to 1.1–1.2 eV for saturation coverage, in good agreement with our calculations. Interestingly, for high coverage, a shallow physisorption well appears suggesting the possibility for trapping molecules in the so-called precursor state. In Figs. 1 e) and f) we show the geometry of this physisorption well. By comparing these panels to Fig.1 d), we observe that the other adsorbates only slightly move towards the physisorbed adsorbate. In the following, we will interchangeably use the names precursor state, trapping, and physisorption state.

We have run Langevin dynamics for the mentioned coverages and laser fluences of 100 J/m^2 and 140 J/m^2. The results of our dynamics for a coverage of 0.58 ML are shown in Fig. 3,

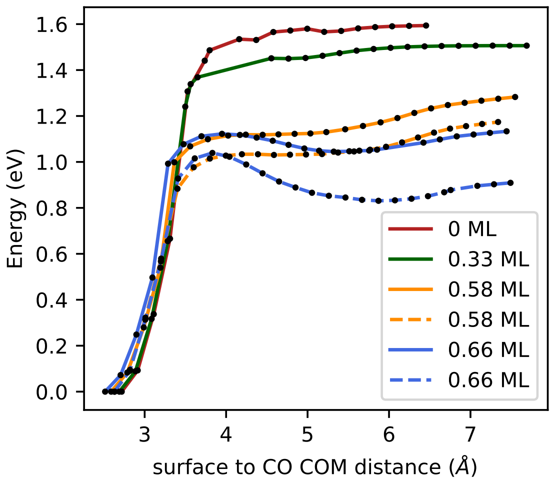

Figure 2: Potential energy of a single CO molecule as a function of the distance of its COM from the surface calculated with our machine learning interatomic potential. For coverages of 0.58 and 0.66 ML, full lines correspond to the CO molecule indicated with a yellow circle and dashed lines to the CO molecule indicated with a purple circle in Fig. 1.

which shows the distance from the surface of the COM of all CO molecules as a function of time. Corresponding figures for coverages of 0.33 ML and 0.66 ML are shown in Figs. S4 and S5. As the laser pulse reaches the surface at the time of 1.16 ps, molecules gain energy (see adsorbate temperatures in Figs. S1 and S2) and the distribution of CO molecules' positions become wider. The average CO COM distance to the surface decreases as molecules move from the on-top of Ru atom position towards more coordinated sites such as bridge and hollow sites, in accordance with previous six-dimensional dynamics.[4] As in Ref. 4, some molecules desorb. Unlike there, however, interestingly, some molecules get trapped at an elevated COM distance from the surface of around 6 Å, as particularly evident from the COM density enhancements in this area for both the COM distance and the logarithmic population plots. Even though the potential energy surface for this coverage does not show a clear physisorption well (for a single desorbing molecule at T=0 K) according to Fig. 2, orange line, molecules can be dynamically trapped.

Since the free energy F of the molecule as a function of distance from the surface z is proportional to logarithm of probability $P(z)$ of finding the molecule at z [i.e., $F(z) \sim -k_B T \ln P(z)$],[32] the distributions shown in Fig. 3 are proportional to the effective free energy of the molecule [also called the potential of mean force (PMF)]. The PMF is a more reliable indicator of a physisorption well or other features of the potential at finite temperature.[1,4] Therefore, the results of Fig. 3 reveal

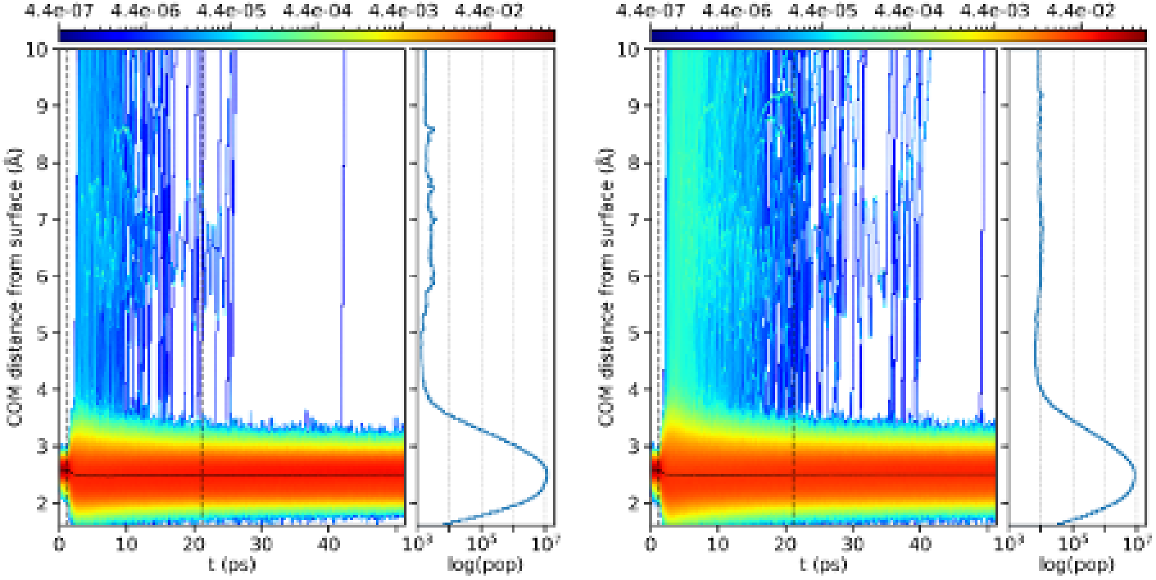

Figure 3: Probability of finding a CO molecule at a given COM distance from surface at a given time (logarithmic scale). The surface coverage is 0.58 ML for fluences of 100 $\mathrm{Jm^{-2}}$ (left) and 140 $\mathrm{Jm^{-2}}$ (right). In the right sub-panels distributions are integrated over a time of 50 ps, giving the ”log(pop)” curves.

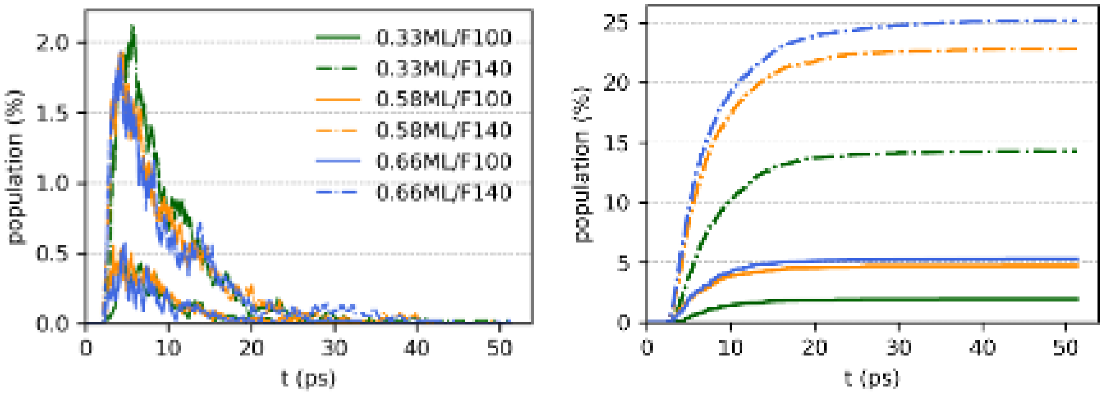

Figure 4: Left panel: trapping probability defined as the probability of finding a molecule with its COM between 4.5 Å and 10 Å from the surface as a function of time. Right panel: desorption probability defined as the probability of finding a molecule with its COM at a distance from the surface larger than 10 Å (right) as a function of time. Full lines are for the fluence of 100 $\mathrm{J/m^2}$ and dashed lines are for the fluence of 140 $\mathrm{J/m^2}$.

the existence of a small physisorption well in the free energy for both 100 $\mathrm{J/m^2}$ and 140 $\mathrm{J/m^2}$. Very similar dynamics and the presence of trapped molecules is seen also for coverages of 0.33 and 0.66

ML for both fluences. Desorption and trapping probabilities as a function of time are shown in Fig. 4. We consider a molecule as desorbed when the distance of its COM from the surface is larger than 10 Å (note that we use nonperiodic boundary conditions in the direction normal to the surface so all molecules that surpass this distance remain in the vacuum because the potential has a finite range). Molecules are in the trapping zone when their COM distance from the surface is between 4.5 Å and 10 Å. These criteria are arbitrarily broad and trapping includes molecules that are directly desorbing, but it reflects the experiments that also cannot distinguish between the two within the trapping region. For the studied coverages and fluences, desorption saturates at around 20 ps after the arrival of the laser pulse and at that time the precursor state is almost completely depopulated, as can be seen from the left panel of Fig. 4. As expected, the number of desorbed molecules increases as the fluence is increased and as coverage is increased since higher fluence increases the energy of molecules and higher coverage decreases the desorption energy. Interestingly, the trapping probability increases with increasing fluence but does not vary much with the coverage.

Our results can be compared to experiments.[1–3] The precursor state is detected in experiments for longer times than in our simulations at $>$100 ps, but the maximum population is at delay times of 4-10 ps similar to our simulations.[3] Experimentally, it was roughly estimated that desorption yields are $\sim$10% for fluence of 100 Jm^{-2} and $\sim$30% for fluence of 140 Jm^{-2}.[2] In experiments CO adsorption is performed at room temperature at which saturation coverage is around 0.54 ML.[27] Our results for the desoprtion yield at the similar 0.58 ML coverage for 100 Jm^{-2} and 140 Jm^{-2} fluences are 4.7 ± 0.3% and 22.8 ± 0.6%, respectively. Similarly, in experiments at temperature of 100 K and for fluence estimated to be 91 Jm^{-2},[3] the desorption yield was estimated to 14.5 ± 5%, while our value for 0.66 ML at room temperature and fluence of 100 Jm^{-2} is 5.3 ± 0.3%. These values are in reasonable agreement with experiments considering experimental uncertainties and approximations in the two-temperature model. Based on the different XAS spectra for the two fluences, 100 Jm^{-2} and 140 Jm^{-2}, it was assumed that the precursor state is populated only for the higher fluence while for the lower fluence only frustrated translation/rotation toward more coordinated hollow and bridge chemisorbed states take place. In constrast, the precursor state is also populated at lower fluences in our simulations, but with smaller probabilities. The maximum probability to form a precursor state in our dynamics is found to be around 0.5% for a fluence of 100 Jm^{-2} and around 2% for a fluence of 140 Jm^{-2}. Our results also show the power of atomistic simulations in understanding experimental results as complicated as the total XAS signal that is averaged over many configurations.

Additionally, in Ref. 1, due to 30% reduction in the so-called $\tilde{d}_\pi$ signal it was assumed that 30% of molecules get pumped into the precursor state and that free energies of chemisorbed and precursor states are thus similar. Our dynamics calculations show that the precursor state is much less populated and that the free energy of the precursor state is much higher than the free energy of the chemisorbed state. We suggest that total experimental spectra can be fully explained only by calculating spectra on an ensemble of structures sampled from our dynamics.

We have also performed simulations for a higher fluence of 200 Jm^{-2} shown in Figs. S6 and S7. Desorption yields increase with higher fluence as expected. However, the trapping probabilities are equal to the trapping probabilities for a fluence of 140 Jm^{-2}. Clearly, at higher fluences, molecules easily desorb and trapping does not increase. Trapping is somewhat higher for lower coverages than for high coverages, despite the fact that the T=0 potential (see Fig. 2) favours trapping for higher coverages. One should keep in mind that coverage is rapidly changing locally during the dynamics as molecules easily diffuse on the surface, creating regions of high local coverage that may give rise to the shallow physisorption minimum in the free energy for all coverages and fluences. In Fig. 5 and Figs. S8 and S9 we plotted lateral positions of molecules on the surface for fluences of 100 Jm^{-2} and 140 Jm^{-2} for the three coverages, showing the diffusion all over the surface, in qualitative agreement with Ref. 4. For higher fluence and coverages, a significant portion of molecules at times around 7 ps after the arrival of the laser pulse occupy hollow fcc and hcp sites, while for lower fluence molecules dominantly stay around the top site. Occupation of hollow sites agrees well with the population of the so-called new adsorbed state identified in the experimental spectra of Ref. 3.

To prove that adsorbate-adsorbate interactions play a crucial role in trapping the precursor state beside the Fig. 2, we performed dynamics for a single molecule in a $\sqrt{3}\times\sqrt{3}$ Ru(0001) unit cell with nominal coverage of 0.33 ML. The results are shown in Fig. S10, which can be directly compared with Fig. S4. It can be seen that in this case there is no trapping, i.e., there is no physisorption well in the free energy. Desorption is also significantly reduced compared to the supercell dynamics, demonstrating that previous theoretical calculations in small supercells tend to underestimate desorption as recently it has also been observed for hydrogen associative desorption from Ru(0001).[15]

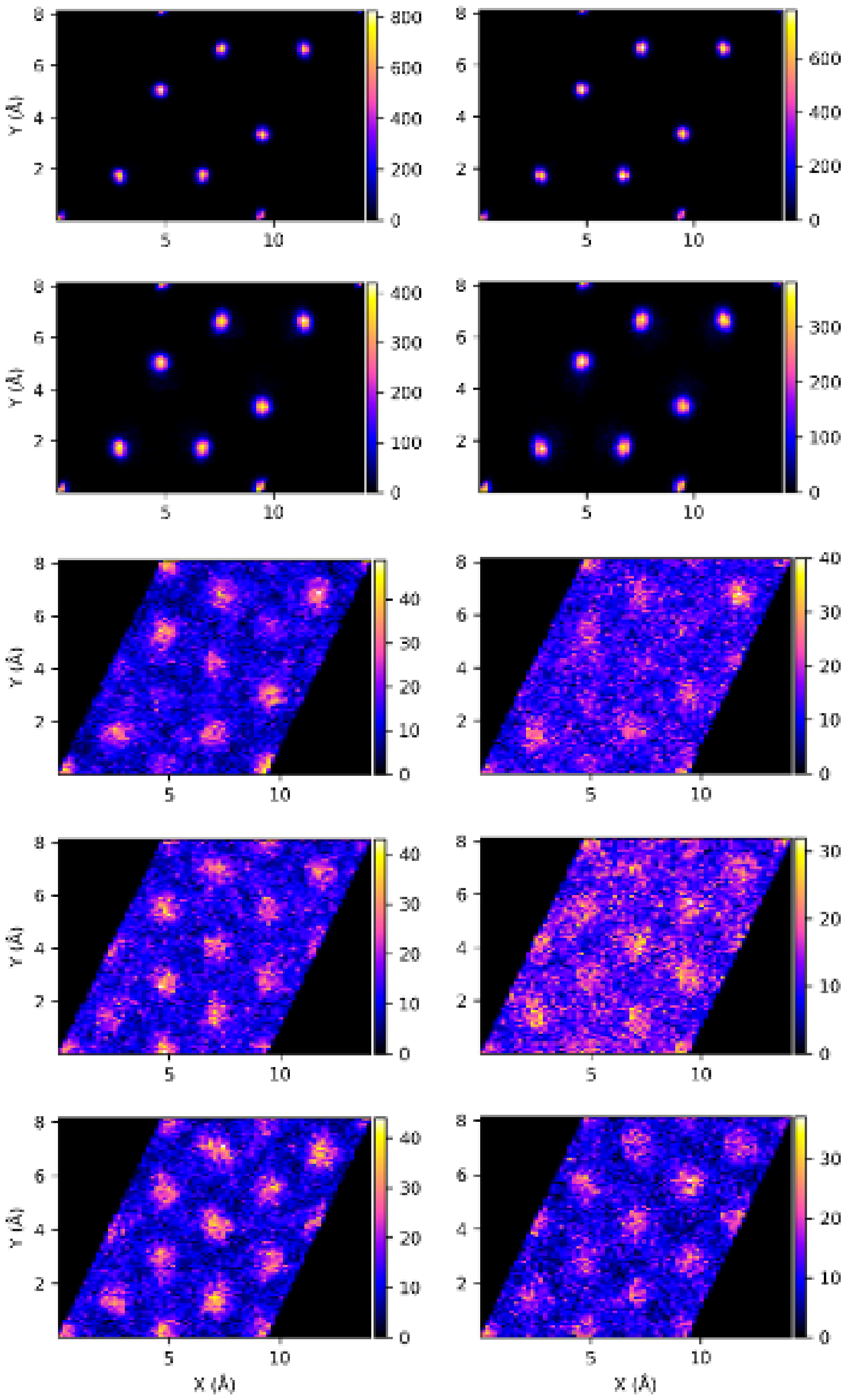

Figure 5: Distribution of (X,Y) values for the C atoms in all trajectories for two fluences, 100/140 Jm^{-2} (left/right), for different times (from top to bottom at -0.1 ps, 2 ps, 5 ps, 7 ps and 30 ps). Coverage is 0.58 ML.

IV. CONCLUSIONS

In conclusion, ultrafast pump-probe experiments are a powerful tool to monitor reactions in real time. However, disentangling the obtained spectra often requires theoretical input. Laser pulse induced dynamics of CO on Ru(0001) is a paradigmatic example where pump probe experiments have found evidence for the existence of a so-called precursor state. However, this precursor state proved to be elusive for atomistic modelling.

We have constructed a new DFT-based machine learning potential energy surface for modelling CO on Ru(0001) that treats all ionic degrees of freedom and is valid for different CO coverages. With the new potential energy surface, we have run molecular dynamics with electronic friction that include laser pulse excitation through electronic and phonon temperatures obtained from the two temperature model. Our dynamics for different coverages and laser fluences capture the elusive precursor state. This state is the result of dynamically trapped molecules with COM distance from the surface of around 6 Å. While the static potential energy surface for a single molecule desorbing from the surface features a shallow physisorption well only for the high coverage of 0.66 ML, the dynamic free energy potential features a physisorption well even for the coverage of 0.33 ML.

Experimentally, a qualitative change in spectra was seen for two fluences of 100 J/m^2 and 140 J/m^2, prompting the conclusion that the precursor state exists only for higher fluences. Our dynamics show that the precursor state can be populated with a lower fluence, too, but with around four times lower probability. Increasing the fluence further increases the desorption but not the trapping in the precursor state as molecules easily desorb at high fluence.

ACKNOWLEDGEMENTS

This work has been supported by Croatian Science Foundation under the project UIP-2020-02-5675 and the European Regional Development Fund within the “Center of Excellence for Advanced Materials and Sensing Devices” (Grant No. KK.01.1.1.01.0001). JIJ and MA acknowledge financial support provided by the Spanish MCIN/AEI/10.1309/501100011033/ and FEDER Una manera de hacer Europa (Grant No. PID2022-140163NB-I00), Gobierno Vasco-UPV/EHU (Project No. IT1569-22), and the Basque Government Education Department IKUR program, also co-funded by the European NextGenerationEU action through the Spanish Plan de Recuperación, Transformación y Resiliencia (PRTR). PS acknowledges financial support by CRC/SFB 1636 of "Deutsche Forschungsgemeinschaft" – project ID 51094390 within project A03.

AUTHOR DECLARATIONS

Conflict of Interest

The authors have no conflicts to disclose.

Author Contributions

Bruno Mladineo: Methodology, Software, Validation, Formal analysis, Investigation, Data Curation, Writing - Original Draft, Visualization; J. Iñaki Juaristi: Methodology, Writing - Review & Editing Maite Alducin: Methodology, Writing - Review & Editing; Peter Saalfrank: Methodology, Writing - Review & Editing; Ivor Lončarić: Conceptualization, Methodology, Software, Resources, Writing - Original Draft, Supervision, Project administration, Funding acquisition

DATA AVAILABILITY STATEMENT:

The machine learning interatomic potential and the training dataset are openly available in Zenodo at https://doi.org/10.5281/zenodo.14589354.

SUPPLEMENTARY MATERIAL:

Supplementary Material includes additional figures (Figs. S1-S10) (PDF).

REFERENCES

[1] M. Dell'Angela, T. Anniyev, M. Beye, R. Coffee, A. Föhlisch, J. Gladh, T. Katayama, S. Kaya, O. Krupin, J. LaRue, *et al.*, "Real-time observation of surface bond breaking with an x-ray laser," Science **339**, 1302–1305 (2013).

[2] M. Beye, T. Anniyev, R. Coffee, M. Dell'Angela, A. Föhlisch, J. Gladh, T. Katayama, S. Kaya, O. Krupin, A. Møgelhøj, *et al.*, "Selective ultrafast probing of transient hot chemisorbed and precurso states of co on ru (0001)," Physical Review Letters **110**, 186101 (2013).

[3] H.-Y. Wang, S. Schreck, M. Weston, C. Liu, H. Ogasawara, J. LaRue, F. Perakis, M. Dell'Angela, F. Capotondi, L. Giannessi, *et al.*, "Time-resolved observation of transient precursor state of co on ru (0001) using carbon k-edge spectroscopy," Physical Chemistry Chemical Physics **22**, 2677–2684 (2020).

[4] R. Scholz, G. Floß, P. Saalfrank, G. Füchsel, I. Lončarić, and J. I. Juaristi, "Femtosecond-laser induced dynamics of co on ru(0001): Deep insights from a hot-electron friction model including surface motion," Physical Review B **94**, 165447 (2016).

[5] A. Luntz, M. Persson, S. Wagner, C. Frischkorn, and M. Wolf, "Femtosecond laser induced associative desorption of h 2 from ru (0001): Comparison of "first principles" theory with experiment," The Journal of Chemical Physics **124**, 244702 (2006).

[6] G. Füchsel, T. Klamroth, S. Monturet, and P. Saalfrank, "Dissipative dynamics within the electronic friction approach: The femtosecond laser desorption of H_2/D_2 from ru(0001)," Physical Chemistry Chemical Physics **13**, 8659–8670 (2011).

[7] J. I. Juaristi, M. Alducin, R. D. Muiño, H. F. Busnengo, and A. Salin, "Role of electron-hole pair excitations in the dissociative adsorption of diatomic molecules on metal surfaces," Physical Review Letters **100**, 116102 (2008).

[8] P. Spiering, K. Shakouri, J. Behler, G.-J. Kroes, and J. Meyer, "Orbital-dependent electronic friction significantly affects the description of reactive scattering of n2 from ru (0001)," The Journal of Physical Chemistry Letters **10**, 2957–2962 (2019).

[9] C. L. Box, Y. Zhang, R. Yin, B. Jiang, and R. J. Maurer, "Determining the effect of hot electron dissipation on molecular scattering experiments at metal surfaces," JACS Au **1**, 164–173 (2020).

[10] I. Lončarić, M. Alducin, P. Saalfrank, and J. Juaristi, "Femtosecond-laser-driven molecular dynamics on surfaces: Photodesorption of molecular oxygen from ag (110)," Physical Review B **93**, 014301 (2016).

[11] I. Lončarić, M. Alducin, P. Saalfrank, and J. I. Juaristi, "Femtosecond laser pulse induced desorption: A molecular dynamics simulation," Nuclear Instruments and Methods in Physics Research Section B: Beam Interactions with Materials and Atoms **382**, 114–118 (2016).

[12] S. Funk, M. Bonn, D. N. Denzler, C. Hess, M. Wolf, and G. Ertl, "Desorption of co from ru (001) induced by near-infrared femtosecond laser pulses," The Journal of Chemical Physics

112, 9888–9897 (2000).

[13] I. Lončarić, G. Füchsel, J. Juaristi, and P. Saalfrank, "Strong anisotropic interaction controls unusual sticking and scattering of co at ru (0001)," Physical Review Letters **119**, 146101 (2017).

[14] P. Liu, J. Wang, N. Avargues, C. Verdi, A. Singraber, F. Karsai, X.-Q. Chen, and G. Kresse, "Combining machine learning and many-body calculations: Coverage-dependent adsorption of co on rh(111)," Physical Review Letters **130**, 078001 (2023).

[15] S. Lindner, I. Loncaric, L. Vrcek, M. Alducin, J. I. Juaristi, and P. Saalfrank, "Femtosecond laser-induced desorption of hydrogen molecules from ru (0001): A systematic study based on machine-learned potentials," The Journal of Physical Chemistry C **127**, 14756–14764 (2023).

[16] A. Muzas, A. S. Jiménez, J. Ovčar, I. Lončarić, M. Alducin, and J. I. Juaristi, "Absence of isotope effects in the photo-induced desorption of co from saturated pd (111) at high laser fluence," Chemical Physics **558**, 111518 (2022).

[17] A. Serrano Jiménez, A. P. Sánchez Muzas, Y. Zhang, J. Ovcar, B. Jiang, I. Loncaric, J. I. Juaristi, and M. Alducin, "Photoinduced desorption dynamics of co from pd(111): A neural network approach," Journal of Chemical Theory and Computation **17**, 4648–4659 (2021).

[18] I. Žugec, A. Tetenoire, A. S. Muzas, Y. Zhang, B. Jiang, M. Alducin, and J. I. Juaristi, "Understanding the photoinduced desorption and oxidation of co on ru (0001) using a neural network potential energy surface," JACS Au (2024).

[19] S. Sinha, B. Mladineo, I. Loncaric, and P. Saalfrank, "Multidimensional neural network interatomic potentials for co on nacl (100)," The Journal of Physical Chemistry C (2024).

[20] S. Batzner, A. Musaelian, L. Sun, M. Geiger, J. P. Mailoa, M. Kornbluth, N. Molinari, T. E. Smidt, and B. Kozinsky, "E (3)-equivariant graph neural networks for data-efficient and accurate interatomic potentials," Nature Communications **13**, 2453 (2022).

[21] A. Musaelian, S. Batzner, A. Johansson, L. Sun, C. J. Owen, M. Kornbluth, and B. Kozinsky, "Learning local equivariant representations for large-scale atomistic dynamics," Nature Communications **14**, 579 (2023).

[22] G. Kresse and J. Furthmüller, "Efficient iterative schemes for ab initio total-energy calculations using a plane-wave basis set," Physical Review B **54**, 11169 (1996).

[23] G. Kresse and D. Joubert, "From ultrasoft pseudopotentials to the projector augmented-wave method," Physical Review B **59**, 1758 (1999).

[24] R. Jinnouchi, F. Karsai, and G. Kresse, "On-the-fly machine learning force field generation: Application to melting points," Physical Review B **100**, 014105 (2019).

[25]M. Dion, H. Rydberg, E. Schröder, D. C. Langreth, and B. I. Lundqvist, "Van der waals density functional for general geometries," Physical Review Letters **92**, 246401 (2004).

[26]A. Tetenoire, J. I. Juaristi, and M. Alducin, "Insights into the coadsorption and reactivity of o and co on ru (0001) and their coverage dependence," The Journal of Physical Chemistry C **125**, 12614–12627 (2021).

[27]Q. Chen, J. Liu, X. Zhou, J. Shang, Y. Zhang, X. Shao, Y. Wang, J. Li, W. Chen, G. Xu, *et al.*, "Unveiling structural evolution of co adsorption on ru (0001) with high-resolution stm," The Journal of Physical Chemistry C **119**, 8626–8633 (2015).

[28]D. E. Starr and H. Bluhm, "Co adsorption and dissociation on ru (0001) at elevated pressures," Surface Science **608**, 241–248 (2013).

[29]R. Scholz, S. Lindner, I. Lončarić, J. C. Tremblay, J. I. Juaristi, M. Alducin, and P. Saalfrank, "Vibrational response and motion of carbon monoxide on cu(100) driven by femtosecond laser pulses: Molecular dynamics with electronic friction," Physical Review B **100**, 245431 (2019).

[30]A. H. Larsen, J. J. Mortensen, J. Blomqvist, I. E. Castelli, R. Christensen, M. Dułak, J. Friis, M. N. Groves, B. Hammer, C. Hargus, E. D. Hermes, P. C. Jennings, P. B. Jensen, J. Kermode, J. R. Kitchin, E. L. Kolsbjerg, J. Kubal, K. Kaasbjerg, S. Lysgaard, J. B. Maronsson, T. Maxson, T. Olsen, L. Pastewka, A. Peterson, C. Rostgaard, J. Schiøtz, O. Schütt, M. Strange, K. S. Thygesen, T. Vegge, L. Vilhelmsen, M. Walter, Z. Zeng, and K. W. Jacobsen, "The atomic simulation environment—a python library for working with atoms," Journal of Physics: Condensed Matter **29**, 273002 (2017).

[31]H. Pfnür, P. Feulner, and D. Menzel, "The influence of adsorbate interactions on kinetics and equilibrium for co on ru (001). ii. desorption kinetics and equilibrium," The Journal of Chemical Physics **79**, 4613–4623 (1983).

[32]M. E. Tuckerman, *Statistical mechanics: theory and molecular simulation* (Oxford university press, 2023).